



Author(s) Kallio, Pasi; Ritala, Tuukka; Lukkari, Mikko; Kuikka, Seppo

Title Injection guidance system for cellular microinjections

Citation Kallio, Pasi; Ritala, Tuukka; Lukkari, Mikko; Kuikka, Seppo 2007. Injection guidance system for cellular microinjections. International Journal of Robotics Research vol. 26, num. 11-12, 1303-1313.

Year 2007

DOI <http://dx.doi.org/10.1177/0278364907084985>

Version Post-print

URN <http://URN.fi/URN:NBN:fi:tty-201412091611>

Copyright Sage Publications 2007

Injection Guidance System for Cellular Microinjections

Pasi Kallio, Tuukka Ritala, Mikko Lukkari and Seppo Kuikka

Institute of Automation and Control

Tampere University of Technology

PL 692, 33101 Tampere, Finland

pasi.kallio@tut.fi

Abstract – This paper presents a novel injection guidance system that assists an operator in the microinjection of living adherent cells. The system includes a micromanipulator, an injection system, an impedance measurement device, and control software. The impedance measurement system detects changes in the resistance of an injection capillary during cell injections. From the measurement signal, the software determines parameters that can be used for detecting several injection events such as cell-capillary contact, capillary breakage, and capillary clogging, which are all unavailable in the current microinjection systems. Real cell injection experiments indicate that injection success rates can be significantly increased: from 30–40% without the system to 65% with the system.

KEY WORDS – Micro/Nano Robots, Biomicromanipulation, Intracellular Microinjection, Injection Guidance, Adherent Cells, Automation, Real-time Software

1. INTRODUCTION

Micromanipulation can be defined as manipulation of objects ranging from about one micrometer to a few millimeters in size. It can be performed by either touching the objects physically or without physical contact. In noncontact manipulation, the objects are manipulated using optical, electrical, magnetic, or acoustic energy. A large number of papers have been published especially on optic and electric manipulation: see for example Berns (1998), Arai et al. (1999), Wong et al. (2004), Pesce and De Felici (1995), and Kim et al. (2004) for further references. Noncontact manipulation is an important way of performing micromanipulation, but the work reported in this paper focuses on the contact type of manipulation.

In addition to the method of manipulation, another important definition of micromanipulation relates to the target of manipulation. Microassembly refers to the handling of miniaturized mechanical, electrical, and optical components and their assembly into complete systems. Biomicromanipulation refers to the handling of objects of biomedical interest, such as eukaryotic cells (e.g. mammalian cells), prokaryotic cells (e.g. bacteria), cellular components (e.g. DNA, protein crystals) or tissue samples. Within the last few years, the development of systems for manipulating oocytes in *in vitro* fertilization and transgenics applications has gained a lot of research attention (Sun et al. 2003; Sun, Greminger and Nelson 2004; Gauthier and Piat 2002; Park et al. 2004; Kumar, Kapoor and Taylor 2003; Zhou et al. 2004; and Pillarisetti et al. 2006). Furthermore, research on the manipulation of bacteria and cellular components, such as DNA and protein crystals, has been reported; see for example Arai et al. (2002), Georgiev, Allen and Edstrom (2004) and Ohara et al. (2004).

Oocytes, bacteria, DNA and protein crystals are manipulated in liquid suspension, contrary to most mammalian cells such as neurons, heart cells, liver cells, kidney cells, etc., which need to adhere to a surface to proliferate and therefore need to be manipulated as adherent cells. This poses different challenges to the micromanipulation system. Because of the smaller size of the adherent cells—compared with oocytes—greater positioning and injection accuracies and a better visualization system, for example, are needed. The small size of the cells also results in a need for very fine injection capillaries. Because capillaries thinner than one micrometer are needed, it is very difficult to visually detect the condition of the capillary, a contact with a cell, a correct injection depth, etc. On the other hand, an additional holding capillary is not needed, since the cells adhere to the bottom of the cultivation dish, as illustrated in Fig. 1.

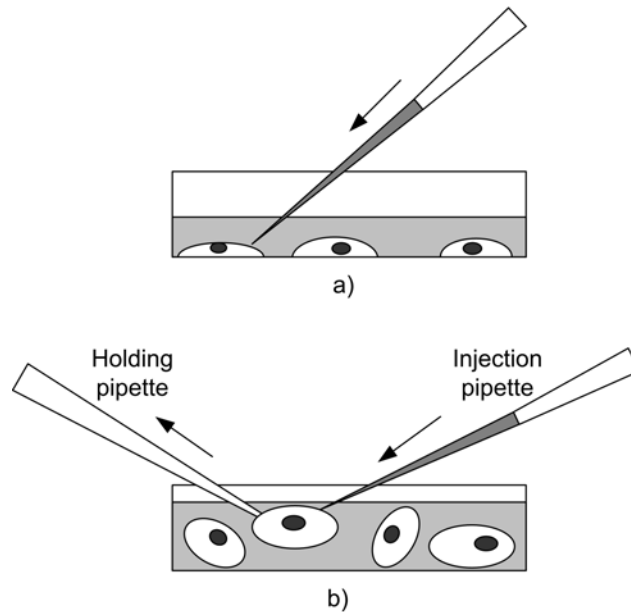


Fig. 1. Microinjection into (a) adherent cells (typically 10–30 micrometers in diameter) and (b) suspended cells (oocytes approximately 100 micrometers in diameter).

An important micromanipulation operation on cells is intracellular injection of small volumes of compounds into cells. A large variety of substances such as dyes, proteins, nucleic acids, drug compounds, or toxins can be injected into cells and their activity studied (Feramisco, Perona and Lacal 1999). Various microinjection methods exist. The most important methods are capillary pressure microinjection, laser beam injection, electroporation, iontophoresis and various endocytosis methods (Davis et al. 2000; Banga, Bose and Ghosh 1999; Lin et al. 2001; Khine et al. 2005; Walker, Dillman and Weiss 1995; and Green et al. 1987). This paper discusses a micromanipulation system designed for *capillary pressure microinjection (CPM)* of single *mammalian cells in adherent cell cultures*, and steps taken toward its full automation.

Capillary pressure microinjection is a mechanical, contact-based method in which a cell membrane is penetrated by a thin microcapillary and a small volume of a compound is delivered from the capillary to the cell upon a pressure pulse. CPM provides the greatest potential for a highly reliable and repeatable injection into single selected cells and for exact control of the volume injected. Furthermore, large molecules can be injected into the cells (Feramisco, Perona and Lacal 1999), and the same end-effector—a microcapillary—can be used in other operations, such as single cell isolation and electrophysiological measurements. Over the last few years, the development of CPM technology has enabled steps toward automation, and research groups are developing automatic microinjectors

(Fukuda and Arai 2000; Tan and Ng 2001; Tan, Ng and Xie 2002; Sun and Nelson 2001; Inoue et al. 2005). Commercial devices such as those provided by Eppendorf, Narishige and Cellbiology Trading are also available; however, even though some systems are already partly automated, a huge amount of manual work is still required by the operator.

An automated system or a system equipped with versatile sensors providing more precise information on the manipulation event would (i) increase the speed of the micromanipulation making it feasible even in high throughput applications, (ii) ease the operation such that a scientist gets the results faster, and (iii) increase the reliability and accuracy of the system such that more reliable results are obtained and success rates are raised. Issues in the automation of living cell manipulation in general and capillary pressure microinjection in particular are discussed in more detail in Kallio and Kuncova (2006), and Kuncova and Kallio (2004), respectively.

One of the biggest bottlenecks for the development of a fully automatic cell injection system has been the lack of information on (i) the contact between a cell and a microcapillary tip and (ii) the condition of the microcapillary. Because of the extremely small size of the capillary tip (less than one micrometer in outer diameter in adherent cell injections), the operator cannot reliably detect when the tip of the capillary is in contact with the cell, when the tip is clogged, or when small breakages of the tip have occurred, and therefore does not know whether the injection is successful.

This paper presents a novel injection guidance system (IGS) that for the first time provides real-time information about cell-capillary contact and capillary condition during adherent cell injections for a microinjection scientist. The injection guidance system consists of an impedance measurement device, detection algorithms, and a graphical user interface. Our previous papers have discussed the hardware development (Lukkari et al. 2004) and the most appropriate indicators of injection events (Lukkari and Kallio 2005). In this paper, we describe the developed detection algorithms, and the application of the injection guidance system to cell injections. The paper is organized as follows: Section 2 discusses the micromanipulation system where the IGS is used. The impedance measurement device that measures changes in capillary resistance during the injections is briefly described in Section 3. An overview of control software is presented in Section 4. Detection algorithms and the injection guidance interface are discussed in Sections 5 and 6, respectively. Sections 7 and 8 present experimental results and Section 9 provides conclusions.

2. MICROMANIPULATION SYSTEM

In this research, the injection guidance system was used in a micromanipulation system developed by the research group. The micromanipulation system consists of four subsystems: a manipulator system, an incubation system, a vision system and a control system. The manipulator system is briefly described in the following.

The manipulator subsystem is composed of a three degrees-of-freedom (DOF) micromanipulator MANiPEN, a coarse one DOF translation stage, an injection/aspiration system, and the impedance measurement device. Fig. 2 depicts the block diagram of the manipulator system. The micromanipulator positions the capillary precisely in cell operations. The coarse positioning device moves the micromanipulator such that the capillary can be placed into and withdrawn from a cell culture well. The injection/aspiration system applies either a positive or negative pressure to the capillary to perform cell injections and aspirations, respectively. The impedance measurement device measures the capillary resistance to provide additional information on the injection to the operator.

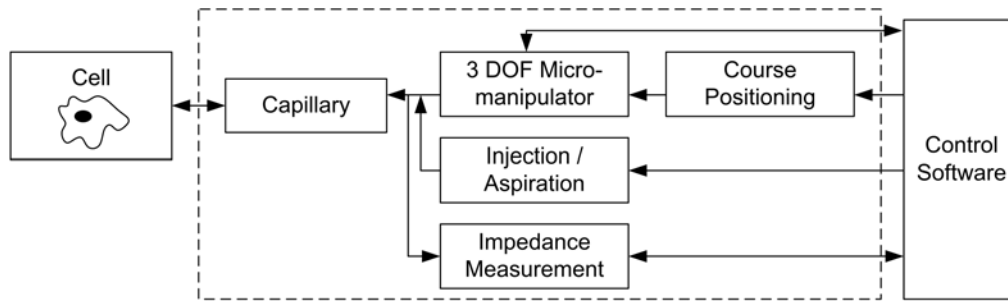


Fig. 2. Block diagram of the manipulator system.

MANiPEN is composed of three actuators organized into a serial structure and provides positioning on orthogonal axes. Motion along the longitudinal axis is executed with a linear drive and along the two transversal axes using two piezoelectric bending actuators. The linear drive comprises two actuators: an electric linear stepper motor for large-range motions and a piezoelectric stack actuator for high-precision short-range movements (Novotny et al. 2002). For enhancing the accuracy of the actuators, PID closed-loop control schemes are utilized. Therefore, the actuators are equipped with position feedback sensors. The linear drive employs an optical linear encoder and the piezoelectric bending actuators are equipped with strain gauges. The manipulator, illustrated in Fig. 3, has a slim pen-like shape that allows for the placement of several manipulators around a microscope, contrary to most current micromanipulators.

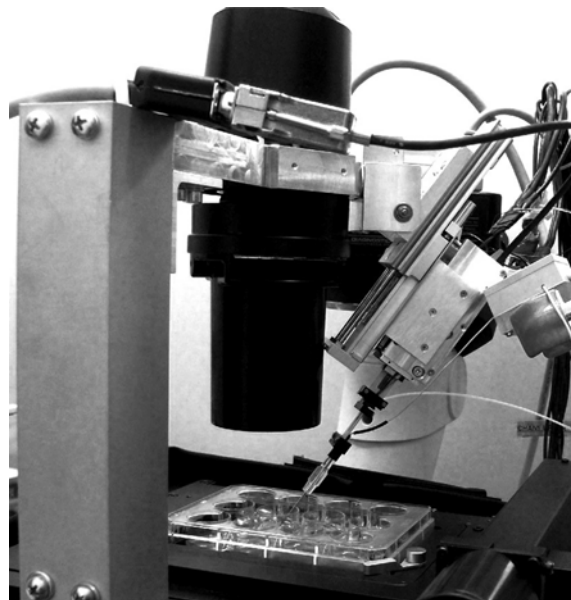


Fig. 3 Photograph of the MANiPEN micromanipulator.

3. IMPEDANCE MEASUREMENT DEVICE

The impedance measurement device utilizes the general principle of a current/voltage clamp circuit (such as presented, e.g., in Sakmann and Neber 1995). The device measures the resistance of the capillary by supplying a known square-wave voltage signal (“stimulus signal”) between a measurement electrode placed inside the injection capillary and a reference electrode placed in a cell culture well and measuring current.

A simplified block diagram of the measurement device is presented in Fig. 4. The *Stimulus Processing and Scaling* block includes adjustable scaling and buffering of the stimulus signal. The stimulus signal is generated with the control software of the manipulator system. The *Current*

Measurement block consists of a sensitive current-to-voltage converter and a differential amplifier. The *Signal Conditioning and Amplification* block includes a low-pass filter and an adjustable output amplifier. The actual system implementation of the impedance measurement device is separated into two parts: a head stage and a control unit. The head stage placed next to the capillary includes the current-to-voltage converter circuit and the control unit includes all the other functions of the device. A more detailed description of the device can be found in Lukkari et al. (2004).

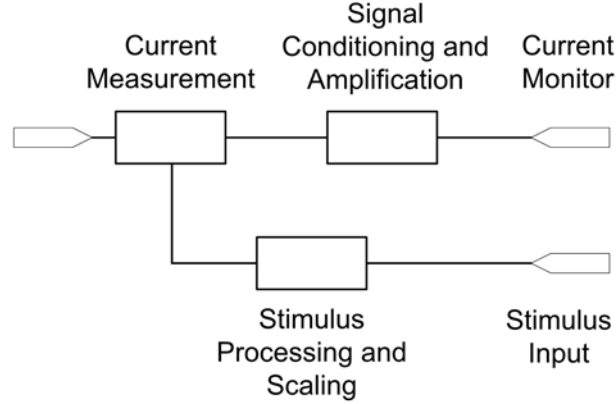


Fig. 4. A simplified block diagram of the impedance measurement device.

An equivalent electric circuit composed of the capillary, the cell and cell medium, and the measurement principle are illustrated in Fig. 5. When the capillary is placed into the medium, mostly the properties of the capillary determine the current. When the capillary is in contact with the cell, also leak resistance, patch resistance, and cell resistance and capacitance are included in the circuit. A transfer function representing electric impedance of the cell-capillary system is given in Equation (1).

$$\frac{U(s)}{I(s)} = Z(s) = \frac{a_1 s + a_0}{b_2 s^2 + b_1 s + b_0}, \quad (1)$$

$$\text{where } a_1 = R_m C_m (R_{leak} R_{patch} + R_{leak} R_p + R_{patch} R_p), \quad a_0 = R_{leak} (R_{patch} + R_m + R_p) + R_p (R_{patch} + R_m),$$

$$b_2 = R_m C_m C_p (R_{leak} R_{patch} + R_{leak} R_p + R_{patch} R_p),$$

$$b_1 = R_m C_m (R_{leak} + R_{patch}) + R_p C_p (R_{leak} + R_{patch} + R_m) + R_{leak} C_p (R_{patch} + R_m), \quad b_0 = R_{leak} + R_{patch} + R_m, \quad R_p \text{ is capillary resistance, } R_{leak} \text{ is leak resistance, } R_m \text{ is membrane resistance, } R_{patch} \text{ is patch resistance, } C_p \text{ is capillary capacitance and } C_m \text{ is membrane capacitance.}$$

This work focuses on using the resistive component of impedance for detecting cell-capillary contact and capillary condition.

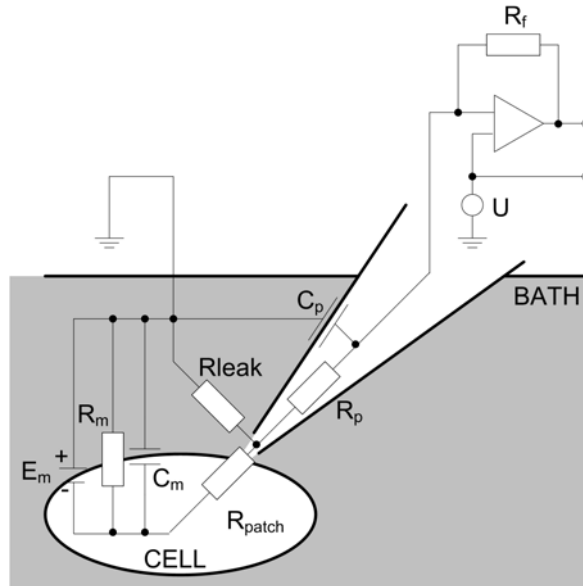


Fig. 5. Illustration of the electric circuit of a cell-capillary system and the measurement principle. Adapted from Johnston and Wu (1997) and Sakmann and Neher (1995).

4. CONTROL SOFTWARE

This section provides an overview of the control software of the manipulator system. It is discussed in more detail in Ritala, Kallio and Kuikka (2006). The software is based on a real-time Linux operating system. The software is fundamentally an operator interface to the micromanipulator and tools attached to it. Using the software, a human operator is capable of moving the micromanipulator in a three-dimensional workspace, and using the other components of the manipulator subsystem. The following sections discuss the selection of the software platform and present an overview of the software structure. Performance issues related to the software are also discussed.

4.1 Operating System

In order to successfully carry out cell manipulation tasks, the precision of the micromanipulator must be in the magnitude of micrometers. In order to enhance the precision of the actuators to a sufficient level, a local closed-loop control scheme is facilitated. The control operations are executed at a (user-selectable) frequency in the order of some kilohertz. Because closed control loops are used, timing of the control operations must be kept precise, and because of the strict timing requirements, it is important to carefully consider the software platform to be used.

Linux is an attractive solution for many software applications because of its wide range of capabilities and large developer community. However, it is a general-purpose operating system incapable of deterministic high-precision timing. Therefore, it is not suitable for high-frequency control applications as such. However, quite a number of Linux-based real-time operating systems are available that provide the required capabilities. After a survey of available systems, the RTAI (Real-Time Application Interface) real-time extension for Linux was chosen as the platform for the control application. The primary reason for choosing RTAI was that it provided good performance measures and a good application programming interface (API).

4.2 Software Structure

On the highest level, the software is divided into two parts: the user interface and the controller. The controller is responsible for executing time-critical control operations and the user interface interacts with the user and relays the commands given by the user to the controller. Both of these have been further divided into several modules, each of which has a distinct task. One of the modules located in the controller is an *Injection Guidance Module* that contains the cell and capillary detection algorithms. The user interface contains a module for illustrating the detection results to the user. These two modules are presented in more detail in Sections 5 and 6, respectively.

4.3 Performance Issues

The timing performance of the implemented system was tested by measuring the interval of successive executions of the control operations in a standard PC equipped with a 2400 MHz Intel Pentium IV. During the tests, no other real-time applications were executed. The timing performance test was repeated with various control frequencies between 1 and 10 kHz. The tests showed that the variation of timing is below $0.5 \mu\text{s}$ at all control frequencies; thus, the timing precision achieved by the software system is sufficient in the intended control frequency range of the software.

5. DETECTION ALGORITHMS

As discussed in Section 3, a square-wave voltage signal has been used as a stimulus signal, thus resulting in a square-wave current measurement signal. In the following, the high level of the square-wave is named as a pulse level and the low level as an offset level, as illustrated in Fig. 6. A pulse amplitude is the difference between the pulse level and the offset level. A reference pulse amplitude is the normal pulse amplitude given by the operator and against which the measured pulse amplitudes are compared.

The detection algorithms were developed by using Matlab[®] to analyze data recorded with the impedance measurement device. Four different indicators in the raw measurement data were studied in the analysis: (i) a change in the pulse amplitude, (ii) a change in the offset level, (iii) a change in the noise at the pulse level and (iv) a change in the noise at the offset level of the square-wave. The most reliable indicator for the cell contact and capillary diagnostics is the change in the pulse amplitude, as discussed in Lukkari and Kallio (2005). The offset is needed in the electrode diagnostics.

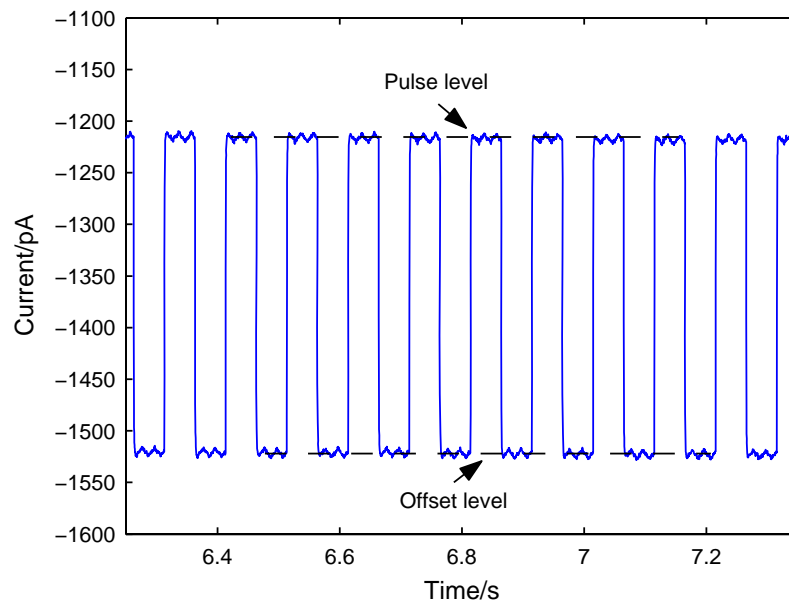


Fig. 6. Illustration of the measurement signal and the terms used.

The detection algorithms executed by the control software perform online cell contact, capillary and electrode diagnostics. They include algorithms for the determination of the two indicators (pulse amplitude and offset) from the raw data, the detection of cell-capillary contact, capillary breakage, capillary clogging, and a time for changing the measurement electrodes using the indicators. The algorithms are presented in Fig. 7.

```

Algorithm contact_measurement
01 raw[d] := read_sensor()

02 if raw[d] - raw[d-1] < -pls_edge_size then
03   pls_start = d - pls_len + s
04   pls_end = d - s
05   ofs_start = d - 2 * pls_len + s
06   ofs_end = d - pls_len - s

07   pulse := mean(raw, pls_start, pls_end)
08   offset := mean(raw, ofs_start, ofs_end)
09   pulses[p] := pulse - offset

10   if ref_count < pulses_in_ref then
11     ref := avg(pulses)
12     incr(ref_count)
13   else
14     if pulses[p] < contact_level * ref then
15       contact := true

16   for i := to pulses_in_break
17     if pulses[p - i + 1] >
18       break_level * ref then
19       incr(b)
20   if b = pulses_in_break then
21     breakage := true

22   if magn(offset) > changing_offset and
23     pulses[p] > changing_pulse then
24     change_electrode := true
25   incr(p)
26   incr(d)

```

Fig. 7. A slightly simplified illustration of the cell contact and capillary detection algorithms.

The online determination of the indicators from the raw data is described in more detail in Section 5.1. The algorithm for the detection of cell-capillary contact is discussed in Section 5.2, the capillary breakage algorithm in Section 5.3, capillary clogging in Section 5.4 and the algorithm for changing the electrodes in Section 5.5. Finally, configuration and reinitialization of the algorithms are discussed in Section 5.6.

5.1 Indicator Signals

At the beginning, the measurement signal is sampled to a buffer *raw* that is capable of storing the samples of a single pulse–offset cycle (row 01). Then, an occurrence of a falling edge of the pulse is sought in row 02. If such an edge is taking place, the starting and ending indices of the pulse part and the offset part of the cycle are calculated in rows 03–06. The lengths of the pulse and offset parts of the cycle are the same given value (*pls_len*). A safety coefficient *s* is used to discard the samples close to the edges of the pulse.

The pulse levels and the offset levels are determined as the mean values of the latest pulse and offset values in rows 07–08. The pulse amplitude is the difference between the offset and the pulse levels (row 09).

If the measurement has been started or a reinitialization command issued, a reference pulse is computed (rows 11–12). Otherwise, the contact detection and capillary diagnostic algorithms are executed in rows 14–24, as described in the next sections.

5.2 Cell-capillary Contact

Cell-capillary contact is detected by reduction in the pulse amplitude. The pulse amplitudes are calculated by subtracting the offset level preceding a pulse from the pulse level (row 09). The calculated pulse amplitude is compared with the reference pulse amplitude *ref* determined by the operator at the beginning of the measurement or later in the measurement when reinitialization is performed. The algorithm calculates the ratio between the measured pulse amplitude and the reference pulse amplitude and provides it to the operator as a percentage. If the reduction is larger than a given limit, an alarm on cell contact is given to the operator through the user interface (rows 14–15). Fig. 8 presents a raw signal measured with the contact detection device in cell-capillary contact. A pulse amplitude recorded in a cell injection experiment will be depicted in Section 7.1.

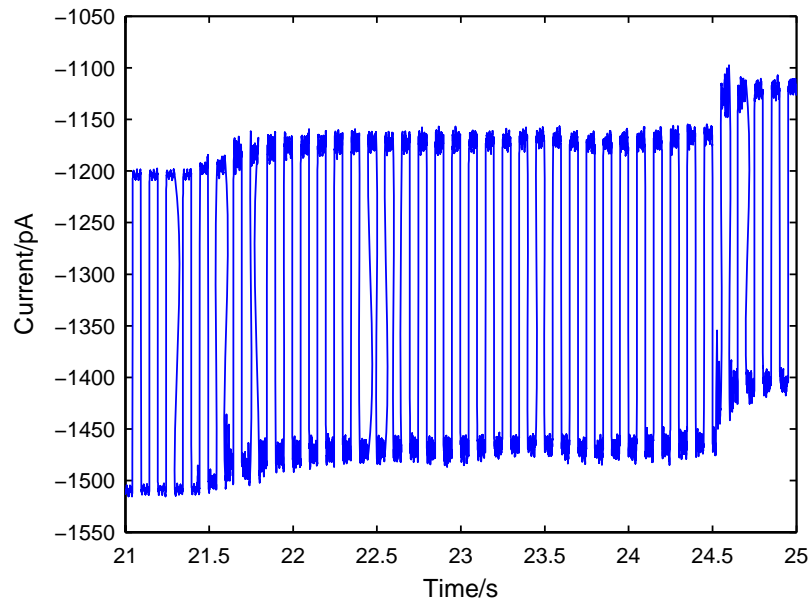


Fig. 8. Raw measurement signal at the beginning of cell-capillary contact.

5.3 Capillary Breakage

Capillary breakage is detected by an increase in the pulse amplitude using a breakage detection limit (*break_level*) in rows 16–21. Several consecutive pulses, the number of which can be specified (*pulses_in_break*), are used in order to avoid faulty detection of the breakage when the capillary is leaving the cell. Faulty detection could otherwise take place, since the offset level usually increases when the capillary leaves the cell, resulting in a temporary increase in the pulse amplitude. If the capillary breakage is small, the reference pulse can be determined again by reinitialization and the injection procedure can be continued. If the capillary breakage is large, the system advises the user to change the capillary.

5.4. Capillary Clogging

Clogging of the capillary can be detected by reduction in the pulse amplitude. If the contact detection device indicates a decreased pulse amplitude, and from the position of the micromanipulator it is known that the capillary is not in contact with the cell, it can be concluded that the capillary is clogged and the capillary should be cleaned or changed.

5.5 Changing Electrodes

When the electrodes are used for some time, they usually lose their chloride coating and their half-cell potentials change, resulting in an increased offset. The detection algorithm gives a notification to change the electrodes when the offset level exceeds a given limit (*changing_offset*) while the pulse amplitude is below the specified limit *changing_pulse*.

5.6 Configuration and Reinitialization

An important part of the contact detection software is the capability of the user to set the parameters of the detection algorithms. The user may set the sensitivity limits of contact detection (*contact_level*), breakage detection (*break_level*), and capillary changing detection (*changing_offset* and *changing_pulse*), as well as the length of the pulse (*pls_edge_size*). In addition, the number of pulses used for calculating the reference pulse amplitude (*pulses_in_ref*) and detecting capillary breakage (*pulses_in_break*) may be set.

Reinitialization is used for computing a new value for the reference pulse. The reinitialization algorithm simply sets the *ref_count* variable to zero, such that the contact detection algorithm will compute a new value for the reference pulse amplitude.

6. INJECTION GUIDANCE INTERFACE

The user interface of the control software consists of several windows. This section briefly presents the injection guidance interface, consisting of three parts: a microinjection trigger mechanism, a contact detection status window, and a contact detection configuration window.

The execution of microinjections must be triggered manually by the operator. After the tip of the capillary has been brought into contact with the cell membrane, the microinjection procedure may be triggered, for example, with a button on a joystick. The role of the contact detection status window is to assist the operator in deciding when to trigger a microinjection. The window visualizes the different aspects of the cell contact detection signal using LED lights, numeric displays and a bar indicator. The window simply illustrates the outputs of the analysis algorithms discussed in Section 5.

The LED lights of the window visualize the status of the capillary. There are lights that alert to contact with a cell, breakage and clogging of the capillary, as well as the need to change the electrodes.

The numeric displays show values determined from the measurement signal. They show the latest value of the pulse amplitude, the current reference pulse value, and the first measured value of the pulse amplitude (with this value the operator may observe a long-term trend in the pulse amplitude during several microinjections). The bar indicator visualizes the current pulse amplitude compared with the value of the reference pulse amplitude as a percentage change. If for some reason the trend of the pulse amplitude changes significantly, the operator may reinitialize the reference value of the pulse with a reset button.

The cell contact analysis may be modified with a variety of parameters. In addition to the parameters discussed in Section 5.6, the amplitude and the frequency of the stimulus signal can be changed.

7. MEASUREMENT RESULTS

The developed injection guidance system was tested in real cell injections. The testing was done with a human breast cancer cell line, MCF-7. The injection solution used was fluorescein isothiocyanate (FITC) diluted in KCl and the cell culture medium was Leibowitz L-15 (Sigma-Aldrich, Munich, Germany; L5520), which requires no pH adjustment with carbon dioxide. The medium was supplemented with 5% dextran-coated, charcoal-stripped treated fetal bovine serum (FBS), penicillin-streptomycin, 10 ng/ml insulin, 1 nM 17β -oestradiol, and 2 mM L-glutamine.

The amplitude of the square-wave stimulus pulses used was 5 mV and the frequency 10 Hz. The sampling frequency used in the recordings was 2 kHz. Experiments on cell-capillary contact detection are introduced in Section 7.1, the detection of capillary breakage in Section 7.2, and capillary clogging in Section 7.3.

7.1 Cell-Capillary Contact

Cell-capillary contact is detected by reduction in the pulse amplitude, as discussed in Section 5. The amplitude of the pulses (electric current) reduces as the total resistance of the cell-capillary system increases in cell-capillary contact. In Fig. 4 and Equation (1), R_{leak} describes the leaking resistance of the contact. Its value depends on the tightness of the contact. If the contact is not tight, a great portion of current flows from the capillary to the medium through the gap between the capillary and the cell. If the contact is tight, the gap is small and the amount of leaking current is significantly lower. In the model, the value of R_{leak} is high and considerably more current is flowing through the cell. Therefore, the strength of the contact corresponds with an increase in the resistance R_{leak} and thus, as a reduction in the pulse amplitude, as illustrated in Fig. 9. If the contact is very gentle or the capillary barely touches the cell, the pulse change is small. If the capillary is pushed more to the cell the changes in the pulse amplitude become much larger (even 50% or greater). The cell type, the capillary tip, and the angle of the capillary, among other variables, have an effect on pulse amplitude reduction. However, variation in amplitude is very small when the capillary is not in contact with a cell: therefore, the parameters can be adjusted such that contact is detectable by a very small change. Contact can be detected even with 5% reduction in the amplitude without false detection. Fig. 9 shows an example of the percentage change in the pulse amplitude in a cell-capillary contact. Typically 5% changes or greater have been considered as contact.

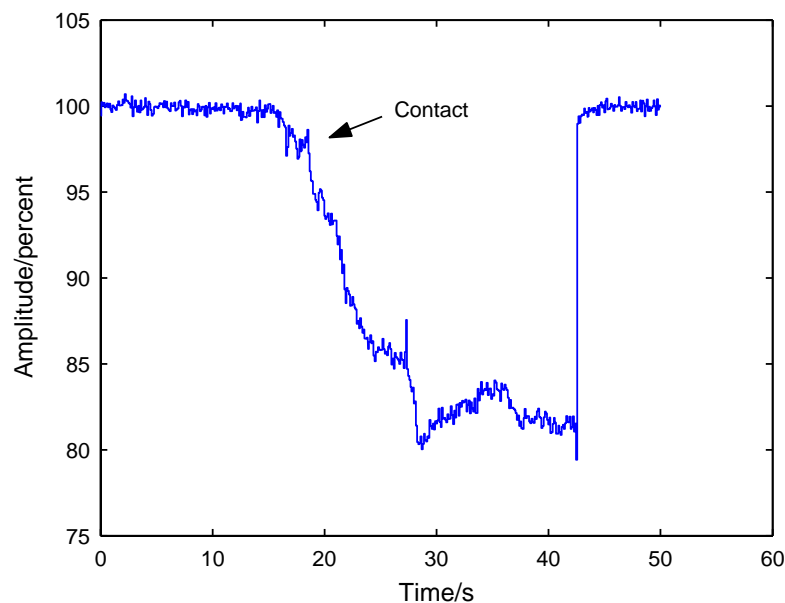


Fig. 9. Decrease in the pulse amplitude in a cell-capillary contact.

To illustrate the resistance change in a contact (see Fig. 10), the resistance value is calculated using measured current pulses and the known supply voltage. At the beginning of the illustrated measurement, the resistance value of the capillary is approximately 15.6 M Ω . When the capillary is in contact with the cell, combined cell-capillary resistance has increased to approximately 19 M Ω .

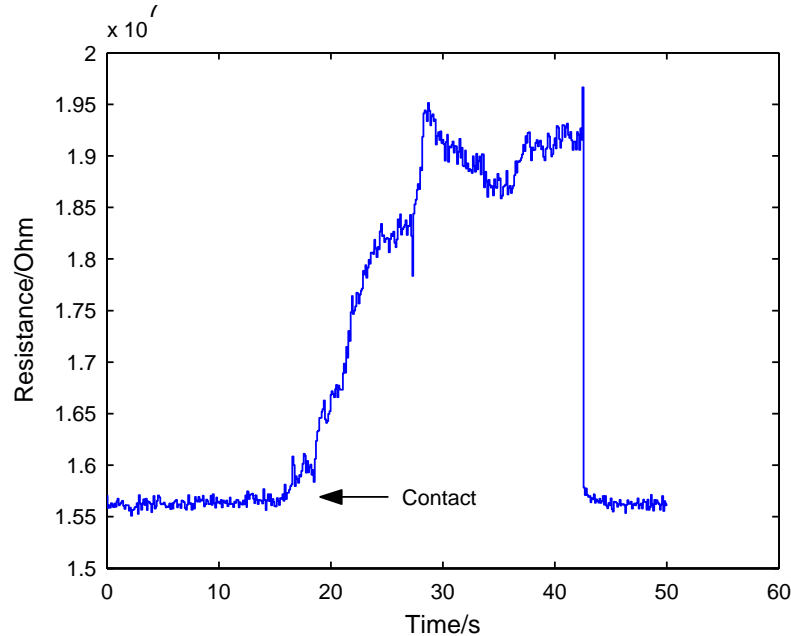


Fig. 10. Change in resistance in a cell-capillary contact.

7.2 Capillary Breakage

When the capillary is in contact with the cell, only the parameters R_p and C_p in Fig. 4 and Equation (1) are considered to be included in the electric circuit. When the size of the tip increases - i.e. the capillary breaks - the capillary resistance R_p decreases. Therefore, breakage of the capillary is detected by an increase in the pulse amplitude. The amplitude of the pulses increases as the resistance of the capillary decreases in capillary breakage. Even if the breakage is very small (even barely visible with a microscope at 200x magnification), the increase in amplitude is relatively large and the breakage can be easily detected. Similarly to the cell-capillary contact measurement, the detection limits can be set as low as 5%. Fig. 11 shows an example of the change in the pulse amplitude when the capillary is broken so much that it needs to be changed.

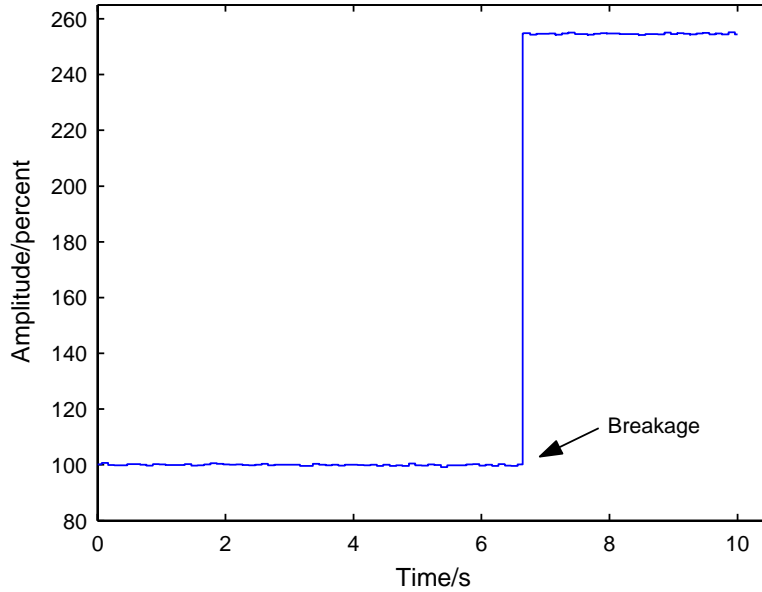


Fig. 11. Increase in the pulse amplitude in a capillary breakage.

7.3 Capillary Clogging

When the size of the tip decreases - i.e. the capillary gets clogged - the capillary resistance R_p increases. This can be detected by a reduction in the pulse amplitude while the capillary is not in contact with a cell. Fig. 12 illustrates a percentage change in the pulse amplitude recorded when a capillary got clogged in a cell injection. When the capillary was moved away from the cell after the injection, the pulse amplitude was smaller than before the injection differently from a typical case shown in Fig. 9. Reduced pulse amplitude during the injection indicates a clogged capillary.

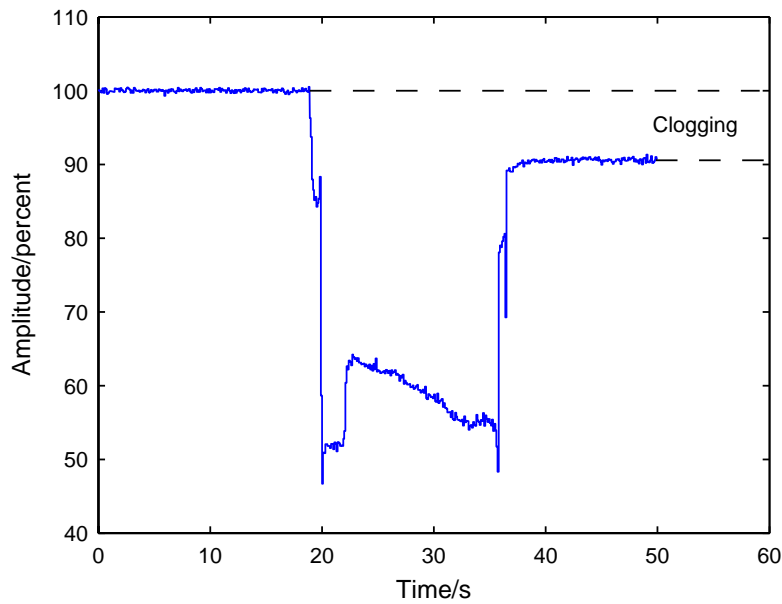


Fig. 12. Pulse amplitude variation in a cell-capillary contact in a cell injection where the capillary became clogged during the injection.

8. INJECTION EXPERIMENTS

The significance of the developed injection guidance system was studied in cell injections. Injection success was first determined without and then with the injection guidance system.

In the experiments, fluorescent dye FITC was injected into MCF-7 cells. Before experimental studies, cells were cultivated for 2–3 passages in phenol red free DMEM/F12 medium supplemented with 5% dextran-coated, charcoal-stripped treated fetal bovine serum (FBS), penicillin-streptomycin, 10 ng/ml insulin, and 1 nM 17 α -oestradiol (Gibco Invitrogen Life Sciences, Paisley, UK). The day before microinjection, cells were plated in 12-well plates at a density of 5×10^4 - 7×10^4 cells per well. Cells were allowed to attach overnight. For transportation of the cells from the University of Tampere Medical School to the injection site and for the experiments, the medium was replaced with L-15 Leibovitz medium (Sigma-Aldrich, Munich, Germany), which requires no pH adjustment with carbon dioxide, supplemented with 5% dextran-coated, charcoal-stripped treated FBS, penicillin-streptomycin, 10 ng/ml insulin, 1 nM 17 β -oestradiol, and 2 mM L-glutamine. Fluorescent dye FITC was used as an injection substance, since a successful injection is easily detected using a fluorescent light after the injection.

Two injection methods have been tested: a “penetration method” and a “contact method”. The penetration method is the conventional “stabbing” method used by current semiautomatic CPM systems (Pepperkok and Saffrich 2001; Ansorge 1988). In this method, the capillary is lowered until a contact between the cell membrane and the capillary is detected visually. The capillary is then rapidly moved a few micrometers along its longitudinal axis to penetrate the cell, and finally, an injection pressure pulse is applied. The contact method is similar to the so-called SLAM (Soft Lipid Assisted Microinjection) method, where the tip of the capillary is coated with lipid bilayer and a contact with the cell membrane is achieved without penetrating the membrane by building up a special aqueous channel (Laffaffian and Hallett 1998). Our experiments have confirmed that when contact between the cell and the capillary is visually detected, the capillary is actually already located inside the cell. Therefore, in our contact method the pressure pulse is applied without the penetration movement of the capillary.

In the experiments, cells were first injected using both methods without the injection guidance system, and the method that resulted in lower performance was then used with the IGS. The injections were performed by an engineering student with strong experience in using the system, not by a professional cell injection scientist. In the experiments, the operator made the decisions concerning injection based on the information provided by the IGS. Fig. 13 illustrates the FITC injection and Table 1 summarizes the results of the experiments. See Extension 1 for video illustration of the injection.

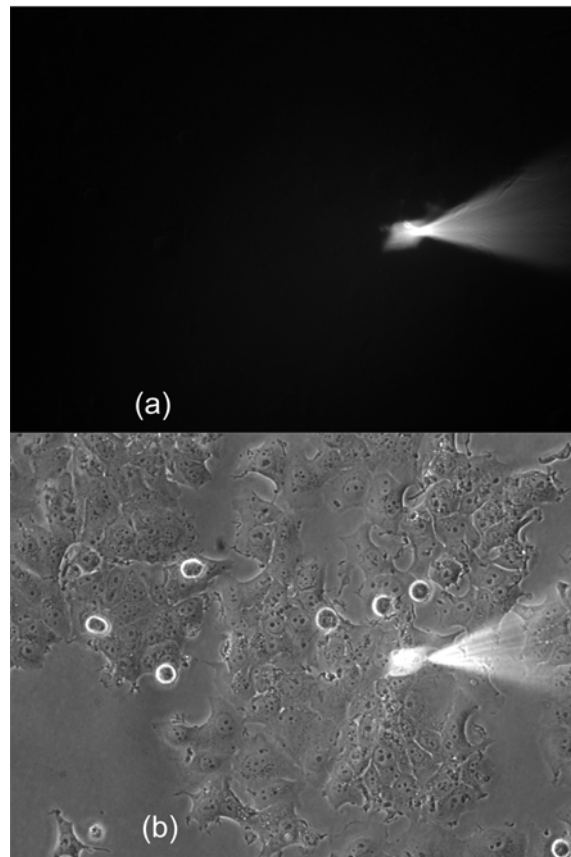


Fig. 13. Injection of fluorescein isothiocyanate into MCF-7 cells: (a) illustration of the injection using only fluorescent light, (b) using both fluorescence and phase contrast.

Table 1: Comparison of success rates of different injection methods.

Method	Number of injected cells	Number of successful injections	Injection success rate
Penetration injection without IGS*	88	35	40 %
Contact injection without IGS*	58	17	30 %
Contact injection with IGS*	55	36	65 %

* IGS = the developed injection guidance system

As can be seen, when the injection guidance system was used, the injection success rate was raised to 65%, which is significantly higher than the 30% and 40% success rates achieved without the system.

9. CONCLUSIONS

This paper presented a novel injection guidance system to assist an operator in the microinjection of living adherent cells. The system is able to provide novel information on the injection events in real-time: thus, the system is able to support the operator in such important decisions as (i) when to perform injection, (ii) when to clean the capillary and (iii) when to change it because of clogging or breakage. As a result of the additional novel information, the system is expected to increase success

rates of microinjection. The first experiments with MCF-7 cells (the number of injected cells equals to 55) show a 65% success rate, which is remarkably higher than approximately 30–40% obtained in previous experiments (Kovanen et al. 2005). However, more experiments are needed to validate the improved success rate and to study the effect of the injection guidance system on cell survival and the speed of the injection. Furthermore, future work will include the development of a fully automatic microinjection system based on the developed injection guidance system.

APPENDIX A: INDEX TO MULTIMEDIA EXTENSIONS

The multimedia extensions to this article are at <http://www.ijrr.org>.

Table 2: Index to Multimedia Extensions

Extension	Type	Description
1	Video	Illustration of fluorescein isothiocyanate into MCF-7 cells

ACKNOWLEDGMENTS

This work is partially supported by Grant #102342 of the Academy of Finland and partially by Grant #40538/03 of the National Technology Agency of Finland, Tekes. In addition to the funding organizations and participating companies, the authors wish to thank Ms. Katrin Kovanen of the Institute of Automation and Control for her assistance in conducting the experiments. Furthermore, the authors thank Dr. Marja-Leena Linne of the Institute of Signal Processing at the Tampere University of Technology and Dr. Tuula Jalonen of the Institute of Medical Technology at the University of Tampere for their help and discussions on the development of the impedance measurement device. Finally, the authors thank Professor Timo Ylikomi and Mr. Sami Purmonen of the Cell Research Center at the University of Tampere for their contributions to the biological issues in the research.

REFERENCES

- Ansorge, W. (1988). Performance of an Automated System for Capillary Microinjection into Living Cells. *Journal of Biochemical and Biophysical Methods* 16(4): 283-292.
- Arai, F., Ogawa, M., Mizuno, T., Fukuda, T., Morishima, K. and Horio, K. (1999 October 17-21). Teleoperated Laser Manipulator with Dielectrophoretic Assistance for Selective Separation of a Microbe. *IEEE/RSJ International Conference on Intelligent Robots and Systems*. Kyonjyu, Korea, pp. 1872-1877.
- Arai, F., Sakami, T., Maruyama, H., Ichikawa, A. and Fukuda, T. (2002 May 11-15). Minimally invasive micromanipulation of microbe by laser trapped micro tools. *IEEE International Conference on Robotics and Automation*. Washington DC, USA, Volume 2: 1937-1942.
- Banga, A.K., Bose, S. and Ghosh, T.K. (1999). Iontophoresis and Electroporation: Comparison and Contrasts. *International Journal of Pharmaceutics* 179(1): 1-19.
- Berns, M.W. (1998). Laser Scissors and Tweezers. *Scientific American* 278(4): 52-57.
- Davis, B.R., Yannariello-Brown, J., Prokopishyn, N.L., Luo, Z., Smith, M.R. and Wang, J. (2000). Glass Needle-mediated Microinjection of Macromolecules and Transgenes into Primary Human Blood Stem/Progenitor cells. *Blood* 95: 437-444.
- Feramisco, J., Perona, R. and Lacal, J. C. (1999). *Needle Microinjection: A Brief History*. Microinjection edited by Lacal, Perona, Feramisco. Basel, Switzerland. Birkhäuser Verlag.

- Fukuda, T. and Arai, F. (2000 April 24-28). Prototyping Design and Automation of Micro/nano Manipulation System. IEEE International Conference on Robotics & Automation. San Francisco, USA, pp. 192-197.
- Gauthier, M. and Piat, E. (2002). An Electromagnetic Micromanipulation System for Single-cell Manipulation. *Journal of Micromechatronics* 2(2): 87-120.
- Georgiev, A., Allen, P.K. and Edstrom, W. (2004 September 28 - October 2). Visually-guided Protein Crystal Manipulation using Micromachined Silicon Tools. IEEE/RSJ International Conference on Intelligent Robots and Systems. Sendai, Japan, Volume 1: 236-241.
- Green, R., Widder, K., Colowick, N. and Kaplan, N. (1987). Drug and Enzyme Targeting, Part B. *Methods in Enzymology* 149. ed. Green, R. and Widder, K.J. Academic Press.
- Inoue, K., Arai, T., Tanikawa, T. and Ohba, K. (2005 November 7-9). Dexterous Micromanipulation Supporting Cell and Tissue Engineering. IEEE International Symposium on Micro-NanoMechatronics and Human Science. Nagoya, Japan, pp. 197-202.
- Johnston D. and Wu S. (1997). *Foundations of Cellular Neurophysiology*. Cambridge, MA, USA. MIT Press.
- Kallio, P. and Kuncova, J. (2006). Capillary Pressure Microinjection of Living Adherent Cells: Challenges in Automation. *Journal of Micromechatronics* 3(3-4): 189-220.
- Khine, M., Lau, A., Ionescu-Zanetti, C., Seo, J. and Lee, L.P. (2005). A Single Cell Electroporation Chip. *Lab on a Chip* 5(1): 38-43.
- Kim, D.H., Haake, A., Sun, Y., Neild, A.P., Ihm, J.-E., Dual, J., Hubbell, J.A., Ju, B.K., Nelson, B.J. (2004 September 1-5). High-throughput Cell Manipulation using Ultrasound Fields. 26th Annual International Conference of the IEEE Engineering in Medicine and Biology Society. San Francisco USA, Volume 4: 2571-2574.
- Kovanen, K., Purmonen, S., Ylikomi, T. & Kallio, P. (2005 November 20-25). Combined Cell Survival and Injection Success Rate in Microinjection of Living Adherent Cells. 3rd European Medical and Biological Engineering Conference. Prague, Czech Republic.
- Kumar, R., Kapoor, A. and Taylor, R.H. (2003 October 27-31). Preliminary Experiments in Robot/human Cooperative Microinjection. IEEE/RSJ International Conference on Intelligent Robots and Systems. Las Vegas, USA, Volume 4: 3186-3191.
- Kuncova, J. and Kallio, P. (2004 September 1-5). Challenges in Capillary Pressure Microinjection, 26th Annual International Conference of the IEEE Engineering in Medicine and Biology Society. San Francisco, USA, Volume 2: 4998-5001.
- Laffaffian, I., and Hallett, M.B. (1998). Lipid-Assisted Microinjection: Introducing Material into the Cytosol and Membranes of Small Cells. *Biophysics Journal* 75(5): 2558-2563.
- Lin, Y-C., Jen, C-M., Huang, M-Y., Wu, C-Y. and Lin, X-Z. (2001). Electroporation Microchips for Continuous Gene Transfection. *Sensors and Actuators B* 79(2-3): 137-143.
- Lukkari, M. J., Linne, M-L., Jalonen, T.O., Karjalainen, M.I., Sarkanen, R. and Kallio, P.J. (2004 September 1-5). Electrical Detection of the Contact between a Microinjection Pipette and Cells. 26th Annual International Conference of the IEEE Engineering in Medicine and Biology Society. San Francisco, USA, Volume 1: 2557-2560.
- Lukkari, M. J. and Kallio, P.J. (2005 June 27-30). Multi-purpose Impedance-based Measurement System to Automate Microinjection of Adherent Cells. 6th IEEE Symposium on Computational Intelligence in Robotics and Automation. Helsinki, Finland, pp. 701-706.

- Novotný, M., Kuncova, J., Kallio, P., Koivo, H.N. (2002 September 11-13). Linear Motor Drive for Micropositioning. International Conference on Machine Automation. Tampere, Finland, pp.251-259.
- Ohara, K., Ohba, K., Tanikawa, T., Hiraki, M., Wakatsuki, S. and Mizukawa, M. (2004 September 28 - October 2). Hands Free Micro Operation for Protein Crystal Analysis. IEEE/RSJ International Conference on Intelligent Robots and Systems. Sendai, Japan, Volume 2: 1728-1733.
- Park, J., Jung, S-H., Kim, Y-H., Byungkyu, K., Lee, S-K., Ju, B. and Lee, K-I. (2004 September 28 - October 2). An Integrated Bio Cell Processor for Single Embryo Cell Manipulation. IEEE/RSJ International Conference on Intelligent Robots and Systems. Sendai, Japan, Volume 1: 242-247.
- Pepperkok, R. and Saffrich, R. (2001). Microinjection and Detection of Probes in Cells. EMBO Practical Course. Website <http://www.embl-heidelberg.de/External/Info/pepperko/MicroinjectionCourse05/>. (Accessed 12.08.05).
- Pesce, M. and De Felici, M. (1995). Purification of Mouse Primordial Germ Cells by Mini-MACS Magnetic Separation System. *Developmental Biology* 170(2): 722-725.
- Pillariseti, A., Pekarev, M., Brooks, A.D., and Desai, J.P. (2006 March 25-26). Evaluating the Role of Force Feedback for Biomanipulation Tasks. 14th Symposium on Haptic Interfaces for Virtual Environment and Teleoperator Systems. Arlington, USA, pp. 11 – 18.
- Ritala, T., Kallio, P. and Kuikka, S. (2006 February 14-16). Real-time Motion Control Software for a Micromanipulator. IFAC Workshop on Programmable Devices and Embedded Systems. Brno, Czech Republic, pp. 304-309.
- Sakmann, B. and Neher, E. (Editors) (1995). *Single-Channel Recording*, 2nd edition. New York, USA, Plenum Press.
- Sun, Y. and Nelson, B.J. (2001 May 21-26). Microrobotic Cell Injection. IEEE International Conference on Robotics and Automation. Seoul, Korea, Volume 1: 620-625.
- Sun, Y., Wan, K.-T., Roberts, K.P., Bischof, J.C. and Nelson, B.J. (2003). Mechanical Property Characterization of Mouse Zona Pellucida. *IEEE Transactions on NanoBioscience* 2(4): 279-286.
- Sun, Y., Greminger, M.A. and Nelson, B.J. (2004 April 26 – May 1). Investigating Protein Structure with a Microrobotic System. IEEE International Conference on Robotics and Automation. New Orleans, USA, Volume 3: 2854-2859.
- Tan, K.K. and Ng, S.C. (2001). Computer-Controlled Piezo Micromanipulation System for Biomedical Applications. *Engineering Science and Education Journal* 10(6): 249-256.
- Tan, K.K., Ng, D.C. and Xie, Y. (2002 June 10-14). Optimal Intra-Cytoplasmic Sperm Injection with a Piezo Micromanipulator. 4th World Congress on Intelligent Control and Automation, Shanghai, China, Volume2: 1120-1123.
- Walker, T., Dillman, N. and Weiss, M.L. (1995). A Constant Current Source for Extracellular Microiontophoresis. *Journal of Neuroscience Methods* 63(1-2): 127-136.
- Wong, P.K., Wang, T-H., Deval, J.H. and Ho, C-M. (2004). Electrokinetics in Micro Devices for Biotechnology Applications. *IEEE/ASME Transactions on Mechatronics* 9 (2): 366-376.
- Zhou, J.W.L., Chan, H-Y., To, T.K.H., Lai, K.W.C and Li, W.J. (2004). Polymer MEMS Actuators for Underwater Micromanipulation. *IEEE/ASME Trans. on Mechatronics* 9(2): 334 – 342.